RSC Advances

PAPER

View Article Online
View Journal | View Issue

Cite this: *RSC Adv.*, 2026, **16**, 7080

An integrated strategy based on LC/MS for the systematic screening of loganin metabolites *in vivo*

Ping Wu,†[a] Hualian Zhu,†[a] Dingli Hu,[b] Yuhua Tan,[b] Sixuan Yang,[b] Yongliang Huang,[a] Kailin Li *[b] and Hui Li*[b]

Loganin is an active compound derived from *Cornus officinalis* Sieb. et Zucc., which has been widely used due to its excellent pharmacological effects including anti-diabetic, anti-inflammatory, neuroprotective, and anti-tumor properties. However, the metabolic process of loganin *in vivo* is insufficiently elucidated until now. Therefore, a metabolic networking cluster combined with multiple data processing techniques based on UHPLC-MS was applied to predict the metabolites of loganin and explore their temporal dynamic change patterns. First, the target ions in the blank and dosed groups were systematically screened using the Compound Discoverer (CD) software. Then, the potential metabolites were identified based on the workflow of CD. Second, a metabolic networking cluster (MNC) was proposed to predict the metabolites of loganin according to the related reports in the literature and existing metabolites of loganin. Third, the establishment of diagnostic product ions (DPIs) was used to preliminarily screen and identify the potential metabolites of loganin. As a result, 2 critical metabolites, including loganin and loganetin, were proposed as networking cluster cores, and a total of 34 metabolites were screened and characterized. Results indicated that loganin primarily underwent the deglucosylation, glucuronidation, demethylation, sulfation, and dehydroxylation reactions and their composite reactions *in vivo*. In addition, most metabolites reached their peak concentration between 0.5 and 1 h and then gradually decreased, indicating that the metabolic process of loganin in rats was relatively rapid. In summary, an integrated strategy was proposed to comprehensively elucidate the metabolic pathways of loganin *in vivo*, which provides a vital reference for research on the metabolism of other compounds.

Received 10th October 2025
Accepted 15th December 2025

DOI: 10.1039/d5ra07753b

rsc.li/rsc-advances

1 Introduction

As an iridoid glycoside compound, loganin is primarily extracted, isolated and purified from the fruit of *Cornus officinalis*, which was recorded in *Shen Nong's Materia Medica* thousands of years ago.[1] It comprises a methyl ester of carboxylic acid and a free hydroxyl group in the aglycone moiety, which is connected to D-glucose through a β-glucosidic bond at the C1 position. Since 2005, the pharmacopoeia of the People's Republic of China has used loganin as a quality control index for the detection of *Cornus officinalis*. Its content is relatively abundant, generally ranging from 0.6% to 2.6%.[2,3] Previous studies have revealed that loganin exhibits a wide range of biological activities including anti-inflammatory,[4] antioxidant,[5] anti-depressant[1] and anti-apoptotic[6] effects. The mechanism of action of loganin as a potential antidepressant has been elucidated. It is reported that loganin can alleviate the dysfunction of the hypothalamus-pituitary-adrenal (HPA) axis, upregulate the expression of the brain-derived neurotrophic factor by increasing the levels of 5-hydroxytryptamine and dopamine, and effectively improve the depressive symptoms of mice exposed to chronic unpredictable mild stress (CUMS).[1] Additionally, loganin can improve the synaptic plasticity of the hippocampal structure of the brain by targeting the protein HINT1, thereby relieving depressive behaviors.[7]

After oral administration, drugs need to undergo a series of biotransformation reactions and are eventually eliminated from the body. This process is accompanied by the exertion of pharmacological effects or the generation of toxic and side effects, providing a key theoretical basis for clarifying the mechanisms of action of drugs *in vivo*.[8,9] It is worth noting that the biological activity of drugs often comes not only from prototype drugs but also from their metabolites. Some metabolites may have better therapeutic effects than the parent drug or they may act through new targets, while others may mediate adverse reactions or detoxification processes.[10] For example, loganin can be converted into the deglycation product loganetin by bacterial glycosidase, which can improve acute kidney injury by inhibiting the TLR4 activity and blocking the JNK/p38 pathway.[11] Therefore, it is very important to systematically study the metabolic characteristics of loganin for its pharmacological action. Previous studies have

[a]*Hospital of Chengdu University of Traditional Chinese Medicine, Chengdu 610075, China*

[b]*School of Pharmaceutical Sciences, Hunan University of Medicine, Huaihua 418000, China. E-mail: 20250941590@bucm.edu.cn; lhi18@163.com*

† These authors contributed equally to the study.

primarily focused on the pharmacokinetic characteristic of loganin and quantification *in vivo*.[12] There is limited research on the metabolites of loganin *in vivo*, and the metabolic profiling remains incomplete. Loganin has potential application prospects for the treatment of depression in clinical settings, and it is essential for the understanding of its metabolic profile *in vivo*. Since there is no systematic analytical strategy to mine and screen loganin metabolites from a complex matrix, research on its metabolites remains challenging.

In recent years, ultra-high-performance liquid chromatography combined with high-resolution mass spectrometry (UHPLC-HRMS) has become an excellent analytical technique for screening and identifying the drug metabolites in biological samples due to the advantages of high resolution, accuracy and sensitivity.[13–15] However, the data generated by LC-HRMS usually involve tens of thousands of compounds including endogenous and exogenous metabolites. It is still facing an inherent bottleneck to accurately screen drug-related metabolites in such massive MS datasets and systematically elucidate their metabolic pathways. In addition, drug-related metabolites are usually present at very low concentrations, while the content of endogenous metabolites is high in biological samples. The mass spectrum or chromatographic signals generated by these endogenous metabolites can cause a high background noise that may cover up the characteristic signals of drug metabolites.[16] Parallel reaction monitoring (PRM) mode is an ion monitoring technology based on high-resolution and high-precision MS, which can selectively detect the target ion, thus obtaining the information of all fragment ions of more exogenous metabolites with low response.[17] Furthermore, the primary and secondary metabolites generated under the action of specific metabolic enzymes still have structural correlation with the parent drug after entering the body. The mass differences between the parent drug and its metabolites can serve as a key for identifying the chemical structures of metabolites and analyzing the metabolic pathways of the parent drug. In this study, a metabolic networking cluster was employed to rapidly predict the metabolites of loganin *in vivo* and visualize its metabolic pathways. The Compound Discoverer software is accompanied by multiple data processing techniques including an extracted ion chromatogram (EIC), a mass defect filter (MDF), and a product ion filter (PIF), which can comprehensively trace and screen the potential metabolites of loganin in complex biological matrices. In this study, a metabolic networking cluster coupled with multiple analytical techniques based on ultra high performance liquid chromatography quadrupole exactive orbitrap mass spectrometry (UHPLC-Q-Exactive Orbitrap MS) was established to clarify metabolites and metabolic transformation process of loganin *in vivo*. These studies will provide a basis for the clinical application of loganin and offer an effective strategy for metabolite identification.

2 Materials and methods

2.1. Chemicals and materials

Loganin (Batch number AZDD2254) with a purity greater than 98% was purchased from Chengdu Alfa Biotechnology Co., Ltd (Chengdu, China). Loganic acid with a purity greater than 98% was purchased from the National Institutes for Food and Drug Control (Beijing China). Acetonitrile and methanol were both of HPLC grade, provided by Merck (Kenilworth, USA). LC/MS-grade formic acid was purchased from Fisher Scientific (Waltham, MA).

2.2. Animals experiment

Six male Sprague-Dawley rats (200 ± 10 g) were purchased from Hunan Silaikejingda Experimental Animal Co., Ltd (Changsha, China). The animal license number was SCXK (Xiang) 2021–0002. The rats were acclimatized for a week in a controlled room at 20 ± 2 °C with a humidity of 60% ± 15% and kept on a 12 h light/12 h darkness regime. Six rats were randomly divided into two groups: blank group ($n = 3$) and drug group ($n = 3$). Loganin dissolved in normal saline was orally given to the rats in the drug group at a dose of 100 mg kg^{-1}. The dose was selected based on previous pharmacological studies of loganin, which indicated that this dose can exert therapeutic effects while avoiding acute toxicity.[6,18,19] The rats in the control group were given the same volume of normal saline. Before the experiments, all rats were fasted overnight with free access to water. All animal experiments were approved by the Animal Ethics Committee of Hunan University of Medicine (Huaihua, China).

2.3. Sample collection and preparation

First, 0.5 mL blood sample was collected from the posterior orbital venous plexus at 0.25, 0.5, 1, 2, 4, and 6 h after oral administration. The blood was transferred to a heparin-treated EP tube and centrifuged (4000 rpm) for 20 min at 4 °C. The supernatant was collected and stored at −80 °C until analysis. The tissues from the heart, liver, spleen, lung, kidney and brain of each group were collected after blood collection, cleaned with a saline solution, dried with filter paper, and stored at −80 °C.

The plasma samples from the same group were pooled by mixing equal volumes at each time point. In a centrifuge tube, 500 μL mixed plasma was added to three volumes of methanol. Then the mixture was vortexed for 1 minute and centrifuged at 13 000 rpm for 20 minutes at 4 °C to remove the precipitated proteins. The supernatants were transferred and dried under a gentle stream of nitrogen gas at room temperature. After that, the residues were redissolved in 100 μL of 50% methanol and centrifuged for 20 min at 4 °C (13 000 rpm). A 2 μL aliquot of the supernatant was injected into a UHPLC-Q-Exactive Orbitrap MS system for analysis.

Tissues weighing 1 g were added into 2 mL saline solution. After homogenization and centrifugation at 4 °C (13 000 rpm) for 20 min, the 1 mL supernatant was transferred to another EP tube, mixed with 3 mL methanol, and centrifuged at 4 °C (13 000 rpm) for 20 min. Then, the supernatants were dried with nitrogen at room temperature. The residue was redissolved with 100 μL 50% methanol. After centrifugation at 4 °C (13 000 rpm) for 20 min, the 2 μL of supernatant was taken for analysis.

2.4. UHPLC-MS conditions

Analyses were performed using an UltiMate 3000 Ultra Performance Liquid Chromatography system (Thermo Fisher

Scientific, California, USA) and a Q Exactive high-resolution mass spectrometer equipped with an electron spray ionization (ESI) system (Thermo Fisher Scientific, Bremen, Germany). The separation of samples was accomplished using a waters ACQUITY UPLC BEH C18 (2.1 × 100 mm, 1.7 μm) at a flow rate of 0.3 mL min^{-1} at 40 °C. The mobile phase consisted of 0.1% formic acid in water (A) and acetonitrile (B). The gradient elution procedure is as follows: 0–2 min, 98% A; 2–8 min, 98%–90% A; 8–11 min, 90–85% A; 11–16 min, 85–78% A; 16–20 min, 78–70% A; 20–25 min, 70–5% A; 25–26 min, 5–98% A; 26–30 min, 98% A.

Data acquisition was performed on full-scan data-dependent MS/MS (full scan-ddMS^2) and combined with the PRM mode in positive and negative ion modes. The scanning range was *m*/*z* 100–1500. The ESI MS parameters are as follows: sheath gas and auxiliary gas flow rates were 30 and 10 arb; auxiliary heater temperature was 320 °C; ion transport tube temperature was 350 °C; automatic gain control (AGC) was 1×10^6; S-lens RF level was 50; capillary voltage was set as 3.5 kV in the positive ion mode and 3.0 kV in the negative ion mode; resolution of full mass was set as 70 000; insolation window was *m*/*z* 3.5; and stepped normalized collision energy (NCE) was set as 35%.

2.5. Data processing

The data acquisition and processing were performed using a Thermo Xcalibur 4.2 workstation. The parameters were set as follows: C [0–30], H [0–50], O [0–30], S [0–2], and N [0–5]. The accurate mass measurements were set within a mass error of ±10 ppm.

2.6. Preliminary screening of metabolites

The original HRMS data of blank and dosing plasma samples were imported into the Compound Discoverer 3.3 software to extract the characteristic peaks of batch data. The difference between the two groups with regard to metabolites was screened by calculating the average response values of the compounds detected in the blank group and the dosing group. The target ions with average response value ratios greater than 5 and less than 0.5 in the dosing group and the blank group were screened out as potential target metabolites and interfering ions, respectively. Then, the two generated files were imported into the Inclusion and Exclusion ion list of the PRM mode in the Thermo Xcalibur Instrument for targeted MS/MS analysis. In addition, precursor ion and corresponding molecular formula was predicted for each metabolite based on theoretical *m*/*z* values and adduct ion forms, including $[M + H]^+$, $[M + Na]^+$, $[M + NH_4]^+$, $[M - H]^-$, and $[M + HCOO]^-$. The retention time and MS information of loganin and its metabolites were analyzed using the Xcalibur Qual Browser software to eliminate the interference of addition ions in the identification of loganin metabolites.

2.7. Construction of metabolic networking clusters

A comprehensive metabolic profile of loganin was established based on the existing metabolites *in vivo* or *in vitro* and the computer-aided metabolic prediction platform, such as BioTransformer (https://biotransformer.ca/). It systematically characterized multiple metabolic pathways, including Phase I (oxidation, reduction, and hydroxylation) and Phase II (glucuronidation, sulfation, and methylation), and meticulously elaborated the precise changes in molecular formula and characteristic mass transfer (Δ *m*/*z*) during the metabolic process. On this basis, the metabolic networking clusters of loganin were constructed using the Cytoscape 3.10 software through complex network analysis techniques based on exact mass differences (Δ *m*/*z* ± 10 ppm).

2.8. In-depth prediction of metabolites

The mol file of parent drug structure was imported into the compound library of the Compound Discoverer 3.3 software, and then the raw data of dosing plasma and blank plasma were also imported into this software. The blank group was set as the background for the deduction of endogenous components. The workflow of "MetID w Stats Expected w Fish Scoring and Background Removal" was selected, and 8 kinds of Phase I and 6 kinds of Phase II metabolic reactions were set. Other parameters were as follows: max steps: 0.5 min; mass error: 5×10^{-6}; minimum mass 100; minimum peak intensity: 5×10^4; and ratio of peak area (dosing group/blank group): >5. The potential metabolites were automatically identified, and then, further screened by combining with the MS/MS spectrum.

3 Results and discussion

3.1. Establishment of the analytical strategy

An analytical strategy combined with the metabolic networking cluster and multiple data processing techniques[20,21] was developed to screen and visualize the metabolites of loganin *in vivo* (Fig. 1). Loganin is an iridoid glycoside, which is formed by the combination of an iridoid with a molecule of glucose. It is preliminarily deduced that loganin could generate loganetin by loss of one glucosyl and loganic acid by removing a methyl during the process of metabolism. Thus, loganin and loganetin were regarded as the networking cluster core, which could produce a variety of metabolites. First, the target ions and potential interfering ions in the blank and dosed groups were systematically screened using the Compound Discoverer software. Subsequently, they were imported into the inclusion and exclusion list of the PRM mode, respectively. This approach allows for the precise acquisition of the MS/MS information of the target ions while effectively eliminating signal interference that may be caused by endogenous metabolites. Moreover, the basic structure of the parent drug is not likely to undergo significant changes during the process of biotransformation, and hence, the diagnostic product ions (DPIs) of loganin standard can be used to predict and elucidate the fragmentation pathways of metabolites of loganin. Second, various metabolic reactions were employed to construct metabolic networking clusters including phase I, phase II and their composite metabolism pathways, such as oxidation (15.9943 Da), reduction (2.0151 Da), hydrolysis (18.0100 Da), glutathionylation (307.0832 Da), glucuronidation (176.0315 Da), sulfation (79.9562 Da), and their composite reactions. The primary

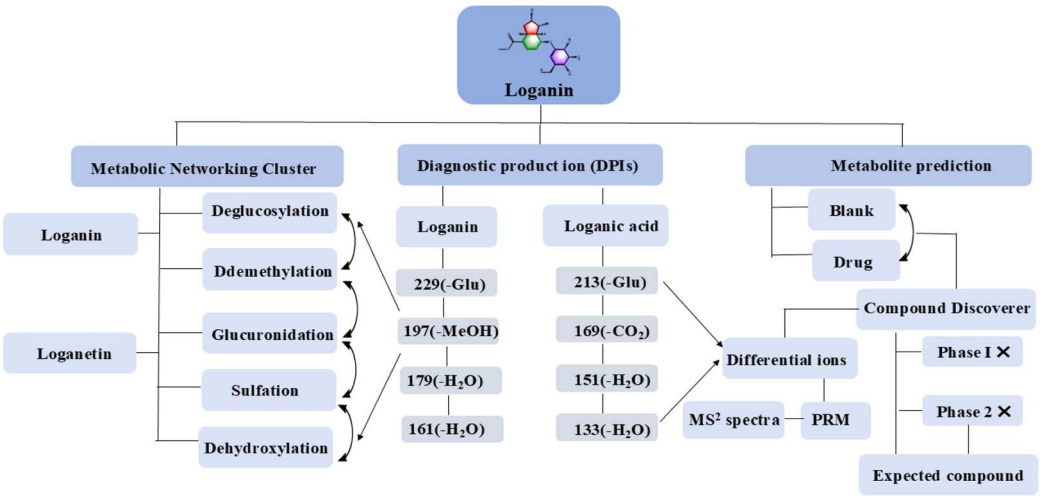

Fig. 1 Workflow of the analytical strategy for the systematic screening of the metabolites of loganin.

metabolites in the metabolic network clusters were screened and identified using EICs and DPIs. By comparing the MS/MS characteristic fragment ions of loganin and its potential metabolites, neutral losses or characteristic fragmentation patterns can be identified. This allows for the inference of the structural modification sites of the metabolites and their possible biotransformation pathways. Then, the raw data of blank and dosed groups were imported into the Compound Discoverer 3.3 software. A list of expected compounds was constructed based on the accurate mass (Δ $m/z \leq 10$ ppm). Fish trace and data mining tools, such as MDF and DPI, were used to screen all the possible metabolites of loganin.

3.2. DPI selection based on the mass fragmentation pathways of loganin and loganic acid

Loganin and loganic acid were used to ascertain DPIs according to the MS^2 fragment information of their standards. They are iridoid glycosides, which are often accompanied by neutral loss of CO, CO_2, H_2O, and glucose residue and easy cleavage of dihydropyran ring and sugar ring. Loganin with the chemical formula $C_{17}H_{26}O_{10}$ showed a precursor ion at m/z 408.1864 $[M + NH_4]^+$, 391.1599 $[M + H]^+$ and 435.1497 $[M - H]^-$. In the positive ion mode, loganin yielded a series of DPIs at m/z 197.0808, 179.0702, 161.0596, 151.0753, 133.0648, and 109.0651 due to the continuous loss of $C_6H_{10}O_5 + CH_2 + H_2O$ (194.0785 Da), $C_6H_{10}O_5 + CH_2 + H_2O + H_2O$ (212.0891 Da), $C_6H_{10}O_5 + CH_2 + 3H_2O$ (212.0891 Da), $C_6H_{10}O_5 + CH_2 + 2H_2O + CO$ (240.0840 Da), $C_6H_{10}O_5 + CH_2 + 3H_2O + CO$ (258.0945 Da), and $C_6H_{10}O_5 + 2CH_2 + 2H_2O + 2CO$ (282.0945 Da). In the negative ion mode, loganin generated DPIs at m/z 227.0924, 127.0392, and 101.0233 after the respective loss of $C_6H_{10}O_5$ (162.0522 Da), $C_{11}H_{19}O_7$ (263.11252 Da), and $C_{13}H_{21}O_7$ (289.12817 Da). Loganic acid showed the deprotonated molecular ion at m/z 375.12967 $[M - H]^-$, which produced the DPIs at m/z 213.0765, 169.0862, 151.0756, 113.0232, and 101.0232 after loss of $C_6H_{10}O_5$ (162.0522 Da), $C_6H_{10}O_5 + CO_2$ (206.0421 Da), $C_6H_{10}O_5 + CO_2 + H_2O$ (224.0526 Da), $C_6H_{10}O_5 + C_5H_8O$ (246.1097 Da) and $C_6H_{10}O_5 + C_6H_8O_2$ (274.10470 Da). The detailed fragment pathways of loganin and loganic acid in the positive and negation ion modes are displayed in Fig. 2.

3.3. Visualization of metabolic networking clusters

Based on the known metabolites of loganin *in vivo* and *in vitro* and a computer-assisted metabolic prediction platform, this study systematically constructed a visual map of the metabolic network cluster of loganin. The network is based on the accurate mass difference ($\Delta m/z \pm 10$ ppm), and the biotransformation relationship between loganin and its metabolites was demonstrated through network analysis technology. In the networking, nodes represented loganin and its Phase I and Phase II metabolites, while the edges characterized metabolic transformation pathways (Fig. 3). The dynamic changes of molecular formula and m/z value during metabolism were accurately analyzed. The metabolite nodes were scaled in size according to their relative abundance. The annotations on the edges contained specific biochemical transformation information. The numbers on the side represented the difference in m/z value between the two connected points. It intuitively presented the transformation path and metabolic cluster association between the parent compound and the metabolic products, thereby revealing its overall metabolic architecture and key metabolic nodes.

3.4. Identification of loganin metabolites

A total of 34 related metabolites of loganin were detected and identified in SD rat plasma, heart, liver, spleen, lung, kidney and brain based on the UHPLC-MS and integrated analytical strategy. Loganin can be easily converted into loganetin after a hydrolysis reaction,[22] and hence, they were particularly divided into metabolites of loganin and loganetin. The detailed metabolite information is given in Table 1, and the EICs of metabolites are shown in Fig. 4.

3.4.1. Metabolites of loganin. Three spots with the precursor ion of 435.1510 $[M + HCOO^-]^-$, 408.1865 $[M + NH_4]^+$

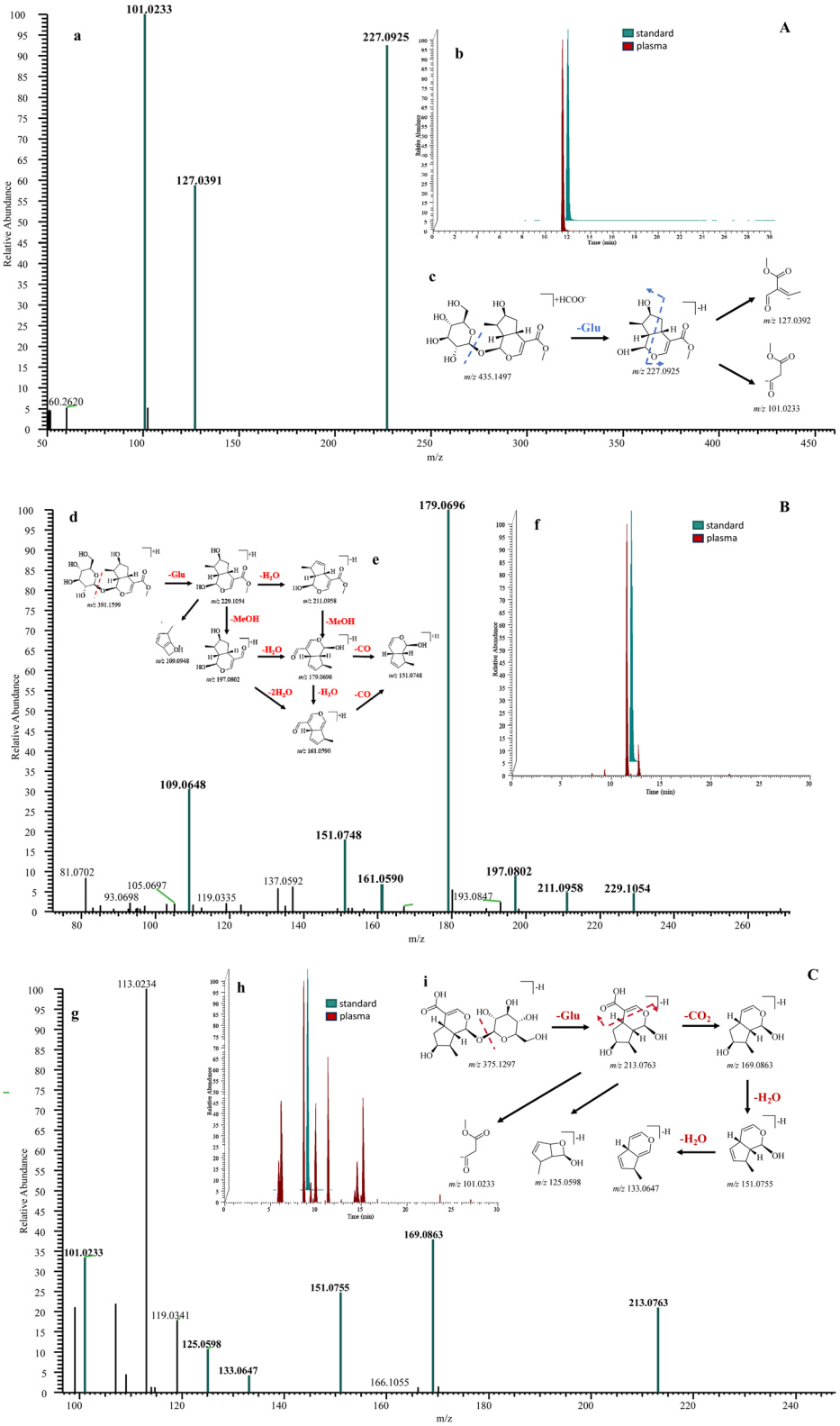

Fig. 2 The EIC and MS spectrum of loganin in the negative (A) and positive (B) ion modes and loganic acid in the negative ion mode (C). (a, d and g) Represent the MS^2 spectra; (b, f and h) represent the EICs of the standard and plasma; and (c, e and i) represent the fragment pathway.

and 391.1600 $[M + H]^+$ were observed, and they have the same retention time. The DPI at *m/z* 227.0924 $[M–H–C_6H_{10}O_5]^-$ by loss of a glucose was observed in the negative ion mode, and 197.0808 $[M + H–C_6H_{10}O_5–CH_2–H_2O]^+$, 179.0702 $[M + H–C_6H_{10}O_5–CH_2–2H_2O]^+$, 161.0596 $[M + H–C_6H_{10}O_5–CH_2–3H_2O]^+$, 151.0753 $[M + H–C_6H_{10}O_5–CH_2–2H_2O–CO]^+$, and 133.0648 $[M +$

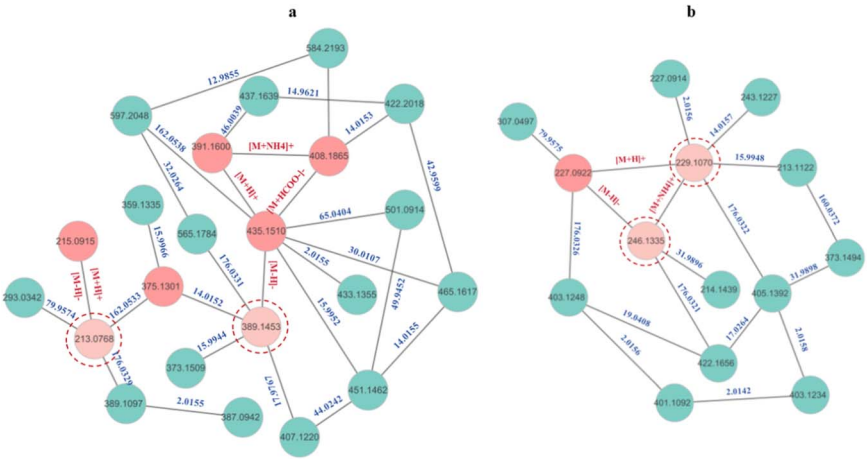

Fig. 3 Metabolic networking clusters of loganin (a) and loganetin (b).

$H–C_6H_{10}O_5–CH_2–3H_2O–CO]^+$ in the positive ion mode, which were consistent with the loganin standard. The loganin (M0) was the core point of metabolic networking, which was closely related to various different molecular masses with 407.1195, 433.1341, 451.1446, 501.0909, 422.2021, 465.1603, 437.1654, 471.1167, 565.1774, 584.2185, and 597.2025 Da according to the MNC (Fig. 3a). The compound with a molecular mass of 433.1355 Da (M15, tR = 11.30 min) was 2.0156 Da less than that of loganin. In the MS/MS spectra, the characteristic fragment ions at *m/z* 225.0767 $[M–H–2H–C_6H_8O_6]^-$ and 101.0232 ($C_4H_5O_3^-$)indicated that dehydrogenation reaction might occur. Consequently, M15 was speculated to be a dehydrogenation product of loganin. M5 and M13 were eluted at 7.98 and 10.63 min and showed $[M + HCOO^-]^-$ ions at *m/z* 451.1462. It was 15.9954 Da more than that of M0, suggesting that the hydroxylation reaction occurred. The DPIs were assigned as *m/z* 243.0875 ($C_{11}H_{15}O_5^-$ + O) $[M–H–C_6H_8O_6]^-$, 225.0767 $[M–H–C_6H_8O_6–H_2O]^-$, 127.0391 ($C_6H_7O_3^-$), and 101.0232 ($C_4H_5O_3^-$). Therefore, M5 and M13 were tentatively identified as the hydroxylation products of loganin. M19 exhibited the $[M + NH_4]^+$ ion at *m/z* 422.2018, which was 14.0161 Da more than that of M0, implying that it might be the methylated product of loganin. In the MS^2 spectra, it produced characteristic ions at *m/z* 211.0967 $[M + H–C_6H_{10}O_5–CH_2–H_2O]^+$, 197.0792 $[M + H–C_6H_{10}O_5–2CH_2–H_2O]^+$, 179.0700 $[M + H–C_6H_{10}O_5–2CH_2–2H_2O]^+$, 161.0595 $[M + H–C_6H_{10}O_5–2CH_2–3H_2O]^+$, 151.0751 $[M + H–C_6H_{10}O_5–2CH_2–2H_2O–CO]^+$, and 133.0645 $[M + H–C_6H_{10}O_5–2CH_2–3H_2O–CO]^+$, hence, M19 was characterized as the methylation product of loganin. M26 displayed a $[M – H]^-$ ion at *m/z* 565.1784 and a $[M + NH_4]^+$ ion at *m/z* 584.2193 corresponding to the 11.91 min. It was 176.0326 Da more than that of M0, manifesting that the glucuronidation reaction might have occurred. The fragment ion at *m/z* 227.0926 $[M–H–C_6H_{10}O_5–C_6H_8O_6]^-$ generated from the loss of glucose in the negative ion mode and *m/z* 229.1070 $[M + H–C_6H_{10}O_5–C_6H_8O_6]^+$, 211.0963 $[M + H–C_6H_{10}O_5–C_6H_8O_6–H_2O]^+$, and 197.0808 $[M + H–C_6H_{10}O_5–C_6H_8O_6–CH_2–H_2O]^+$ in the positive ion mode were observed. Thus, M26 was tentatively identified as a glucuronidation product of loganin. M6 exhibited a $[M – H]^-$ ion at *m/z* 375.1301, and yield characteristic ions at *m/z* 213.0765 $[M–H–C_6H_{10}O_5]^-$, 169.0862 $[M–H–C_6H_{10}O_5–CO_2]^-$, 151.0756 $[M–H–C_6H_{10}O_5–CO_2–H_2O]^-$, and 101.0232 ($C_4H_5O_3^-$), which were consistent with the loganic acid standard. Consequently, M6 was accurately identified as loganic acid. M16 displayed the precursor ion at *m/z* 359.1335, which were 18.0111 Da more than that of M6, and the fragment ions at *m/z* 179.0701 $[M + H–C_6H_{10}O_5–H_2O]^+$, 133.0648 $[M + H–C_6H_{10}O_5–2H_2O–CO]^+$, and 109.0650 ($C_7H_9O^+$). Therefore, M16 was speculated to be a dehydroxylated and dehydrogenated product of loganic acid. M1 and M2 possessed the precursor ions $[M – H]^-$ at *m/z* 293.0342 and 293.0341, which were 79.9573 Da more than that of M3. The characteristic ions at *m/z* 96.9588 ($[HSO_4^-]$), 79.9560 ($[SO_3^{-\cdot}]$) and 213.0764 $[M–H–SO_3]^-$ indicated that the sulfation reaction has occurred *in vivo*. M7 generated the deprotonated molecular $[M – H]^-$ ion at *m/z* 389.1097, and produced fragment ions at *m/z* 213.0770 $[M–H–C_6H_8O_6]^-$, which was 176.0326 Da than that of M3, and 125.0598 ($C_7H_9O_2^-$), 101.0234 ($C_4H_5O_3^-$), 151.0759 $[M–H–C_6H_8O_6–CO_2–H_2O]^-$, and 169.0865 $[M–H–C_6H_8O_6–CO_2]^-$ manifested that the glucuronidation reaction might have occurred.

3.4.2. Metabolites of loganetin. The loganetin, an aglycone of loganin, was detected in plasma. M9 exhibited a $[M – H]^-$ ion at *m/z* 227.0922, which afforded the characteristic ions at *m/z* 127.0390 ($C_6H_7O_3^-$) and 101.0232 ($C_4H_5O_3^-$). The loganetin (M9) was the core point of MNC, which was connected with multiple related masses (Fig. 3b). M10 was 79.9573 Da more than that of M9, which produced a $[M – H]^-$ ion at *m/z* 338.9809. It generated the fragment ion at *m/z* 227.0923 $[M–H–SO_3]^-$, 127.0390 ($C_6H_7O_3^-$) and 101.0232 ($C_4H_5O_3^-$) in the MS^2 spectra. Thus, M10 was tentatively identified as the sulfation product of loganetin. M11 and M21 had a $[M – H]^-$ ion at *m/z* 401.1092, which was 174.0169 Da more than that of M9, indicating that they might be the dehydrogenated and glucuronidated products of loganetin. The fragment ions at *m/z* 225.0768 $[M–H–C_6H_8O_6–2H]^-$ and 101.0233 ($C_4H_5O_3^-$) were observed in the MS/MS spectra, and the fragmentation behavior

Table 1 Identification of the metabolites in rats after the oral administration of loganin

Peak	tR (min)	Theoretical mass *m/z*	Experimental mass *m/z*	Error (ppm)	Formula	Ion mode	MS/MS fragment	Identification
M0[a]	11.51	435.1497	435.1510	0.46	$C_{17}H_{26}O_{10}$	$[M + HCOO^-]^-$	MS^2[435]: 101.0233(100), 127.0392(66), 227.0924(27)	Loganin
	11.52	408.1864	408.1865	0.17	$C_{17}H_{26}O_{10}$	$[M + NH_4]^+$	MS^2[408]: 179.0702(100), 109.0651(33), 151.0753(18), 81.0705(10), 161.0596(8), 197.0808(7)	Loganin
	11.53	391.1599	391.1600	0.25	$C_{17}H_{26}O_{10}$	$[M + H]^+$	MS^2[391]: 149.0233(100), 179.0702(73), 109.0651(40), 151.0753(26), 81.0704(23), 133.0648(14), 161.0596(10)	Loganin
M1	3.81	293.0337	293.0342	1.98	$C_{10}H_{14}O_8S$	$[M - H]^-$	MS^2[293]: 96.9588(100), 213.0769(15), 79.9560(34)	Sulfation of loganetin acid
M2	5.35	293.0337	293.0341	1.46	$C_{10}H_{14}O_8S$	$[M - H]^-$	MS^2[293]: 113.0232(100), 213.0764(23), 96.9588(63), 79.9560(20)	Sulfation of loganetin acid
M3	5.80	215.0914	215.0915	0.37	$C_{10}H_{14}O_5$	$[M + H]^+$	MS^2[215]: 91.0546(100), 109.0650(78), 105.0701(71), 135.0803(13)	Loganetin acid
M4	7.51	213.1121	213.1122	0.30	$C_{11}H_{16}O_4$	$[M + H]^+$	MS^2[213]: 135.0804(100), 79.0548(84), 109.0650(44), 105.0701(39), 121.0649(27)	Dehydroxylation of loganetin
M5	7.98	451.1446	451.1462	1.03	$C_{17}H_{26}O_{11}$	$[M + HCOO^-]^-$	MS^2[451]: 101.0232(100), 127.0391(28)	Hydroxylation of loganin
M6*	8.68	375.1297	375.1301	1.23	$C_{16}H_{24}O_{10}$	$[M - H]^-$	MS^2[375]: 113.0232(100), 89.0231(67), 95.0490(59), 169.0862(43), 101.0232(36), 213.0765(23), 151.0756(22)	Loganic acid
M7	8.73	389.1089	389.1097	1.92	$C_{16}H_{22}O_{11}$	$[M - H]^-$	MS^2[389]: 213.0770(100), 125.0598(56), 101.0234(48), 151.0759(40), 169.0865(34)	Glucuronidation of loganetin acid
M8	10.21	407.1195	407.1220	6.09	$C_{16}H_{24}O_{12}$	$[M - H]^-$	MS^2[407]: 227.0924(57), 101.0232(46), 127.0391(17)	Dihydroxylation and demethylation of loganin
M9	10.24	227.0925	227.0922	−1.26	$C_{11}H_{16}O_5$	$[M - H]^-$	MS^2[227]: 127.0390(100), 101.0232(90)	Loganetin
M10	10.24	307.0493	307.0497	1.10	$C_{11}H_{16}O_8S$	$[M - H]^-$	MS^2[307]: 101.0232(100), 127.0390(77), 227.0923(5)	Sulfation of loganetin
M11	10.61	401.1089	401.1092	0.64	$C_{17}H_{22}O_{11}$	$[M - H]^-$	MS^2[401]: 101.0233(100), 225.0768(30), 123.0441(25), 113.0233(18)	Dehydrogenation and glucuronidation of loganetin
M12	10.61	373.1504	373.1507	0.79	$C_{17}H_{26}O_9$	$[M - H]^-$	MS^2[373]: 75.0075(100), 85.0283(74), 113.0233(71), 71.0126(60), 59.0125(19)	Dehydroxylation of loganin
M13	10.63	451.1446	451.1462	1.17	$C_{17}H_{26}O_{11}$	$[M + HCOO^-]^-$	MS^2[451]: 225.0767(100), 243.0875(27), 179.0706(26), 101.0232(18), 113.0234(16)	Hydroxylation of loganin
M14	11.12	597.2025	597.2048	2.02	$C_{23}H_{36}O_{15}$	$[M + HCOO^-]^-$	MS^2[597]: 227.0924(100), 101.0233(21), 127.0390(11), 209.0819(1)	Dehydroxylation, hydrogenation and glucuronidation of loganin
M15	11.30	433.1341	433.1355	3.34	$C_{17}H_{24}O_{10}$	$[M + HCOO^-]^-$	MS^2[433]: 101.0233(100), 225.0767(83), 123.0442(43)	Dehydrogenation of loganin
M16	11.51	359.1337	359.1335	−0.33	$C_{16}H_{22}O_9$	$[M + H]^+$	MS^2[359]: 127.0390(100), 109.0650(52), 81.0704(46), 151.0753(41), 179.0701(36), 133.0648(16), 123.0805(13)	Dehydroxylation and dehydrogenation of loganic acid
M17	11.51	597.2025	597.2048	2.02	$C_{23}H_{36}O_{15}$	$[M + HCOO^-]^-$	MS^2[597]: 227.0924(100), 101.0233(15), 127.0391(6)	Dehydroxylation, hydrogenation and glucuronidation of loganin
M18	11.53	373.1493	373.1494	0.11	$C_{17}H_{24}O_9$	$[M + H]^+$	MS^2[373]: 179.0702(100), 109.0650(32), 151.0753(16), 133.0647(7)	Didehydroxylation and glucuronidation of loganetin

Table 1 (*Contd.*)

Peak	tR (min)	Theoretical mass *m/z*	Experimental mass *m/z*	Error (ppm)	Formula	Ion mode	MS/MS fragment	Identification
M19	11.53	422.2021	422.2018	−0.55	$C_{18}H_{28}O_{10}$	$[M + NH_4]^+$	MS^2[422]: 179.0700(100), 151.0751(14), 161.0595(6), 133.0645(5), 211.0967(5), 197.0792(2)	Methylation of loganin
M20	11.53	465.1603	465.1617	0.62	$C_{18}H_{28}O_{11}$	$[M + HCOO^-]^-$	MS^2[465]: 225.0757(100), 101.0232(51), 113.0233(47), 123.0441(23), 401.1095(21), 325.0928(20)	Methylation and hydroxylation of loganin
M21	11.57	401.1089	401.1092	0.64	$C_{17}H_{22}O_{11}$	$[M - H]^-$	MS^2[401]: 101.0232(100), 123.0440(24), 225.0763(19)	Dehydrogenation and glucuronidation of loganetin
	11.59	403.1235	403.1234	−0.19	$C_{17}H_{22}O_{11}$	$[M + H]^+$	MS^2[403]: 177.0546(100), 167.0702(52), 195.0652(51), 149.0597(39), 107.0494(22)	Dehydrogenation and glucuronidation of loganetin
M22	11.59	227.0914	227.0914	−0.09	$C_{11}H_{14}O_5$	$[M + H]^+$	MS^2[227]: 149.0596(100), 121.0649(85), 103.0545(57), 107.0494(24), 131.0491(21), 105.0701(10)	Dehydrogenation of loganetin
M23	11.67	597.2025	597.2052	2.64	$C_{23}H_{36}O_{15}$	$[M + HCOO^-]^-$	MS^2[597]: 227.0924(100), 401.1095(39), 113.0233(39), 101.0233(26), 225.0768(24)	Dehydroxylation, hydrogenation and glucuronidation of loganin
M24	11.83	501.0909	501.0914	−1.07	$C_{17}H_{26}O_{15}S$	$[M + HCOO^-]^-$	MS^2[501]: 227.0925(100), 96.9590(52)	Dihydroxylation and Sulfation of loganin
M25	11.84	403.1246	403.1248	0.58	$C_{17}H_{24}O_{11}$	$[M - H]^-$	MS^2[403]: 101.0233(100), 127.0391(57), 113.0233(34), 227.0924(24)	Glucuronidation of loganetin
	11.85	405.1391	405.1392	0.05	$C_{17}H_{24}O_{11}$	$[M + H]^+$	MS^2[405]: 179.0701(100), 109.0650(41), 151.0753(22), 133.0648(13), 137.0596(12), 123.0805(10)	Glucuronidation of loganetin
	11.85	422.1657	422.1656	−0.16	$C_{17}H_{24}O_{11}$	$[M + NH_4]^+$	MS^2[422]: 179.0703(100), 109.0651(9), 211.0964(7), 151.0754(7), 161.0596(4)	Glucuronidation of loganetin
M26	11.91	565.1774	565.1784	1.77	$C_{23}H_{34}O_{16}$	$[M - H]^-$	MS^2[565]: 227.0926(100)	Glucuronidation of loganin
	11.94	584.2185	584.2193	1.35	$C_{23}H_{34}O_{16}$	$[M + NH_4]^+$	MS^2[584]: 179.0702(100), 229.1070(57), 197.0808(37), 109.0651(18), 211.0963(15)	Glucuronidation of loganin
M27	11.94	597.2025	597.2040	0.70	$C_{23}H_{36}O_{15}$	$[M + HCOO^-]^-$	MS^2[597]: 227.0925(100), 101.0232(21), 127.0391(5)	Dehydroxylation, hydrogenation and glucuronidation of loganin
M28	11.98	243.1227	243.1227	−0.21	$C_{12}H_{18}O_5$	$[M + H]^+$	MS^2[243]: 119.0856(100), 125.0597(78), 105.0701(70)	Methylation of loganetin
M29	12.52	243.1227	243.1226	−0.58	$C_{12}H_{18}O_5$	$[M + H]^+$	MS^2[243]: 125.0597(15), 109.0650(15)	Methylation of loganetin
M30	12.52	373.1504	373.1509	1.19	$C_{17}H_{26}O_9$	$[M - H]^-$	MS^2[373]: 75.0075(100), 85.0282(76), 113.0233(60), 71.0125(52), 87.0075(20), 59.0125(13)	Dehydroxylation of loganin
M31	12.56	387.0933	387.0942	2.31	$C_{16}H_{20}O_{11}$	$[M - H]^-$	MS^2[387]: 85.0282(35), 211.0608(35), 181.0135(23), 113.0233(21), 71.0126(15)	Dehydrogenation and glucuronidation of loganetin acid
M32	13.39	214.1438	214.1439	0.56	$C_{11}H_{16}O_3$	$[M + NH_4]^+$	MS^2[214]: 81.0704(100), 95.0859(99), 105.0701(29)	Didehydroxylation of loganetin
M33	16.09	437.1654	437.1639	−3.23	$C_{18}H_{28}O_{12}$	$[M + H]^+$	MS^2[437]: 243.1013(100), 107.0495(65), 133.0648(42), 113.0236(17), 149.0596(4)	Methylation and dihydroxylation of loganin

[a] Identified by comparison with the standard.

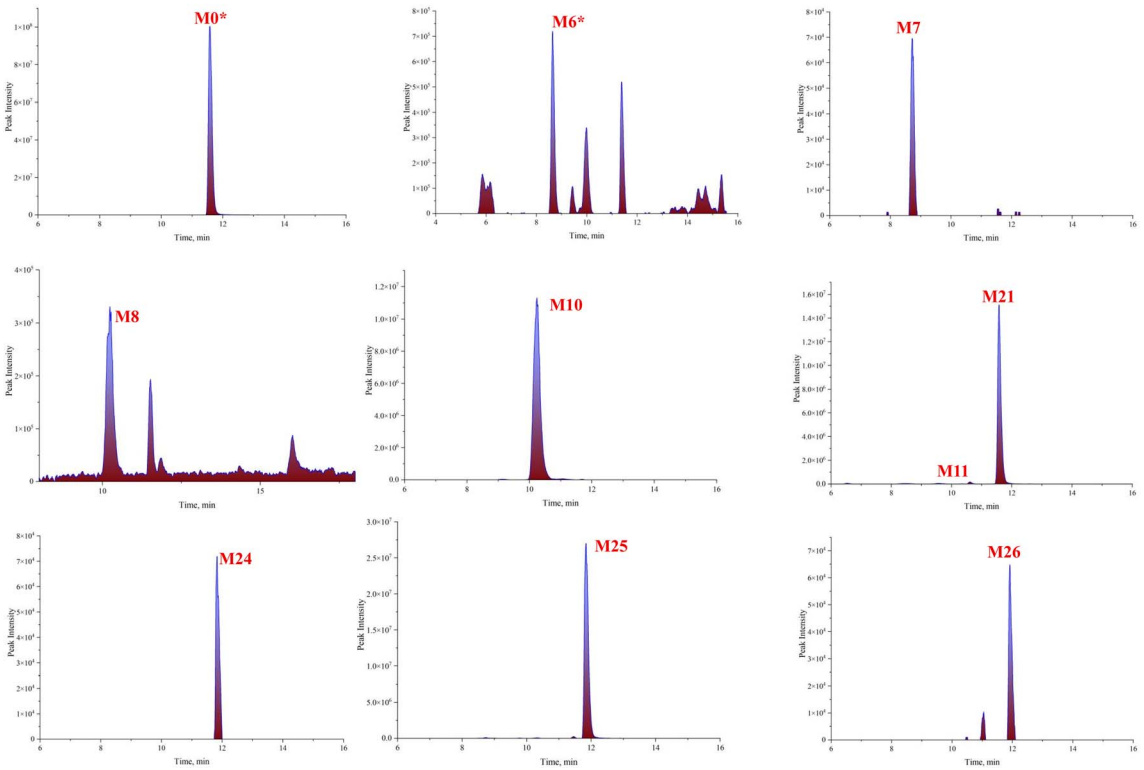

Fig. 4 Representative EICs of the metabolites of loganin identified by LC-MS.

was similar to loganetin. M25 displayed three nodes in MNC, which had the same retention time (11.85 min) and formula ($C_{17}H_{24}O_{11}$). The precursor ion of M25 was at *m/z* 403.1248 $[M - H]^-$, 405.1392 $[M + H]^+$, and 422.1656 $[M + NH_4]^+$, and produced characteristic fragment ions at *m/z* 227.0924 $[M–H–C_6H_8O_6]^-$ 127.0390 ($C_6H_7O_3^-$) and 101.0232 ($C_4H_5O_3^-$) in the ESI^- mode and 211.0964 $[M + H–C_6H_8O_6–H_2O]^+$ and 179.0701 $[M + H–C_6H_8O_6–CH_2–2H_2O]^+$ in the ESI^+ mode.

3.5. Metabolic profiling of loganin

In this study, a total of 34 metabolites (including parent drug) of loganin were detected and identified *in vivo*, and their possible

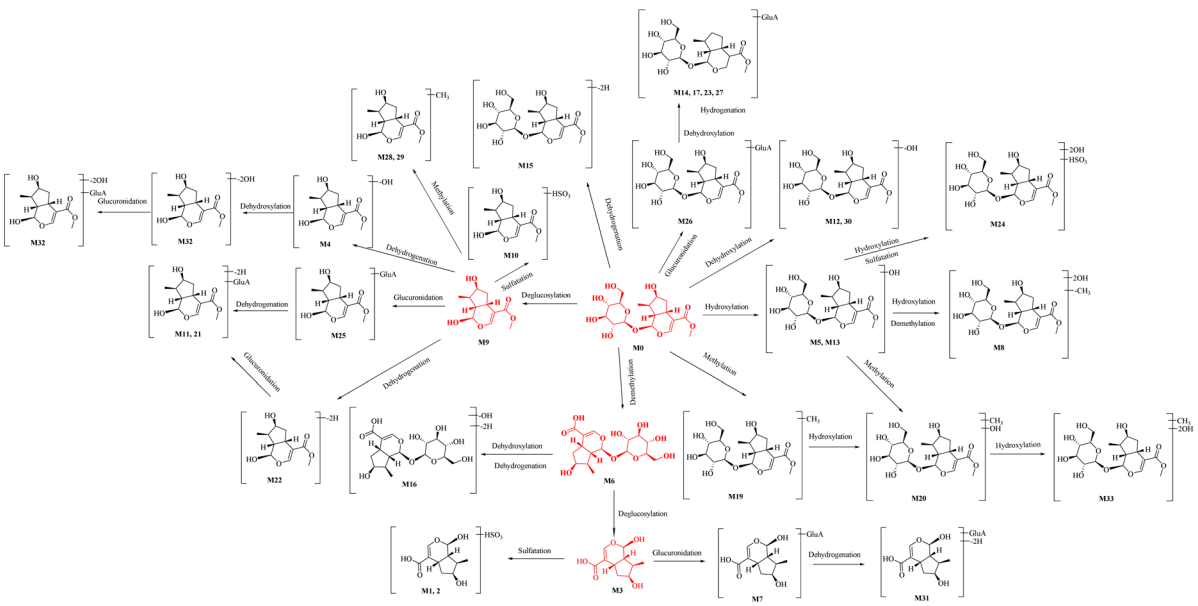

Fig. 5 Metabolic pathways of loganin *in vivo*.

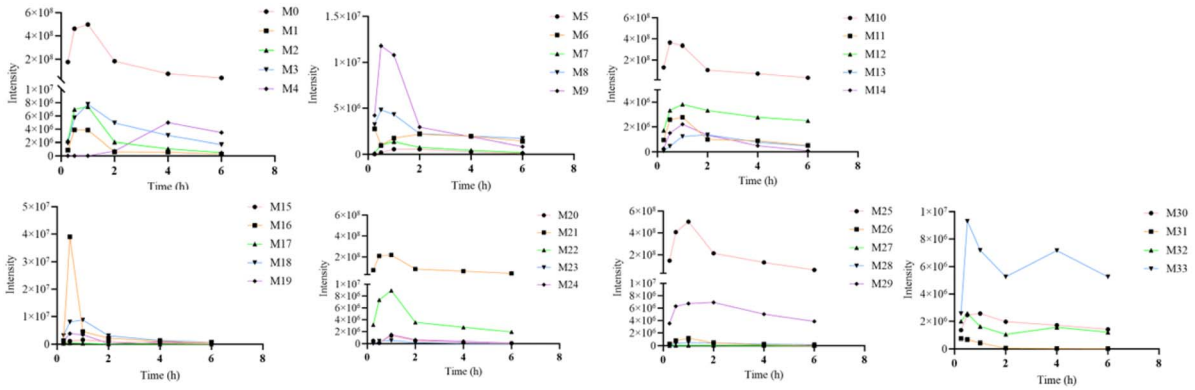

Fig. 6 Time-intensity curves of metabolites.

biotransformation pathways are proposed in Fig. 5. The results indicated that the parent drug first produced three main metabolites, namely, loganetin, loganic acid, and loganetin acid. Preliminary pre-experiment results showed that loganic acid and loganetin acid produced fewer metabolites or have extremely low contents that are undetectable. Therefore, loganin and loganetin were regarded as the core nodes of the MNC for subsequent analyses. Then, the metabolites of loganin were comprehensively explored based on the MNC and various analytical technology. Finally, loganin mainly undergoes deglycosylation, glucuronidation, methylation, sulfation, dehydroxylation, dehydrogenation, and their composite reactions. Among them, the metabolic pathways are dominated by the phase II reaction and their composite reactions, indicating that the increase in drug water solubility is beneficial to the excretion after biotransformation *in vivo*. In addition, this study established the average time-signal intensity curves of metabolites based on the data from 3 rats (Fig. 6). From the descriptive results of this small sample, loganin and most of its metabolites reached signal peaks within 0.5–1 h after administration, followed by a gradual decrease in intensity. This phenomenon preliminarily suggests that the metabolic process of loganin in rats may be relatively rapid, leading to a gradual reduction in the ion intensity of detectable metabolites *in vivo*, and the half-life of these metabolites in the body may be relatively short. The ion intensity changes the patterns of different metabolites. Some metabolites such as M9, M10, M12, M16, M21 and M25 had very high peak values, which gently decreased after

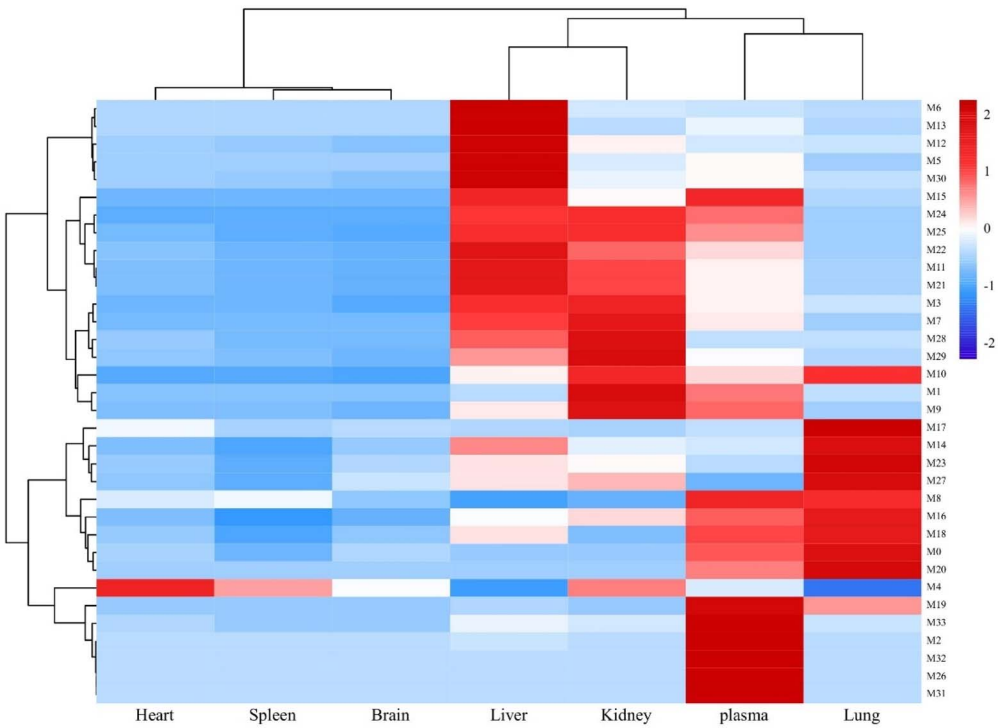

Fig. 7 Heatmap of the peak intensity of 34 metabolites in plasma and tissues.

reaching the peak values, which may suggest that these metabolites were generated in large quantities and had a relatively slow elimination rate in the body. While other metabolites including M1, M2, M7, M8, M11, and M28 reached peaks early with short signal durations, which suggests that they may be rapidly further metabolized or excreted after production. Meanwhile, this study presented the distribution of loganin metabolites in rat plasma and tissues, such as the heart, liver, spleen, lung, kidney, and brain after oral administration in a heatmap (Fig. 7). From the descriptive results of the heatmap, a large area of deep red was observed in the liver region, which preliminarily indicates that most metabolites have high signal abundance in the liver. As the main metabolic organ of the body, the liver is rich in various metabolic enzymes. After loganin enters the body, it is speculated to undergo extensive metabolic transformation in the liver and generate a large number of metabolites, thus the signal abundance of metabolites in the liver is significantly higher than that in other tissues. In contrast, tissues such as the heart, spleen, brain, and lung mostly showed blue or light blue color in the heatmap, suggesting low signal abundance of metabolites in these tissues. This may be attributed to the limited ability of these tissues to take up and metabolize loganin and its metabolites, resulting in a relatively weak metabolic process of loganin in such tissues. However, it should be clearly stated that each group in the animal experiment of this study only included 3 rats, and the small sample size leads to obvious limitations in the study design. This constraint makes statistical analysis of the experimental data impossible, and consequently, reduces the credibility of the results. It must be emphasized that the concentration-time curves of the loganin metabolite are semi-quantitative profiles derived from only three rats and all values are expressed as the mean of the measurements obtained from these three rats. Such semi-quantitative data can only provide a preliminary indication of the metabolic trend of loganin *in vivo* and cannot accurately reveal universal metabolic patterns. Further research will prioritize expanding the sample size and will adopt a more comprehensive pharmacokinetic design to enhance the data reliability and the persuasiveness of the conclusions, thereby remedying the present limitation.

4 Conclusion

In this study, an integrated strategy based on UHPLC-MS was developed for the identification of metabolites of loganin *in vivo*. The loganin and loganic acid standards were used to obtain DPIs, which reversely deduce the possible fragmentation pathway and effectively eliminate ion interference. Finally, a total of 34 metabolites were detected and identified in the rat plasma, heart, liver, spleen, kidney, lung and brain. In addition, the main metabolic reactions included deglucosylation, demethylation, glucuronidation, sulfation, dehydroxylation and their composite reactions. In addition, the metabolism of loganin in rats showed preliminary tissue tendency, and the liver is the main metabolic site. The metabolites were possibly transported by plasma and partially excreted by the kidney, while the participation of the heart, spleen, brain and lung is low. Moreover, loganin was rapidly metabolized in rats and a large number of metabolites were produced in the early stage between 0.5 h and 1 h, followed by the gradual elimination of the metabolites, and the metabolic profiling was different for different metabolites. The study provided a basis for the clinical pharmacological studies of loganin, and the established strategy could be applied to research on the metabolism of other similar compounds.

Sample ethical statement

All animal procedures were performed in accordance with the Guidelines for the Care and Use of Laboratory Animals of Hunan University of Medicine and approved by the Animal Ethics Committee of Hunan University of Medicine (Review Number: 202311034).

Author contributions

Ping Wu: conceptualization, methodology, software, writing original draft. Hualian Zhu: conceptualization, methodology, software, writing original draft. Dingli Hu: investigation, resources, validation. Yuhua Tan: investigation, resources, validation. Sixuan Yang: investigation, resources, validation. Hui Xue: supervision, methodology, software. Kailin Li: writing – review & editing, supervision. Hui Li: writing – review & editing, supervision.

Conflicts of interest

The authors declare that they have no known competing financial interests or personal relationships that could have appeared to influence the work reported in this paper.

Data availability

The findings of this study are available on the metabolic prediction platform Transformer (https://biotransformer.ca/).

References

1 K. Li, Q. Yao, M. Zhang, Q. Li, L. Guo, J. Li, J. Yang and W. Cai, *Arabian J. Chem.*, 2023, **16**, 104875, DOI: 10.1016/j.arabjc.2023.104875.
2 K. Du, J. Li, Y. Bai, M. An, X.-M. Gao and Y.-X. Chang, *Food Chem.*, 2018, **244**, 190–196, DOI: 10.1016/j.foodchem.2017.10.057.
3 G. Cao, Y. Shao, Y. Zhang, X. Cong and B. Cai, *Drugs & Clin.*, 2009, **24**, 272–275.
4 C. Park, H. Lee, C.-Y. Kwon, G.-Y. Kim, J.-W. Jeong, S. O. Kim, S. H. Choi, S.-J. Jeong, J. S. Noh and Y. H. Choi, *Biol. Pharm. Bull.*, 2021, **44**, 875–883, DOI: 10.1248/bpb.b21-00176.
5 Y.-C. Cheng, L.-W. Chu, J.-Y. Chen, S.-L. Hsieh, Y.-C. Chang, Z.-K. Dai and B.-N. Wu, *Cells*, 2020, **9**(9), 1948, DOI: 10.3390/cells9091948.

6 C. H. Park, T. Tanaka, J. H. Kim, E. J. Cho, J. C. Park, N. Shibahara and T. Yokozawa, *Toxicology*, 2011, **290**, 14–21, DOI: 10.1016/j.tox.2011.08.004.
7 C. Xia, G. Zuo, M. Wang, Y. Wang, Y. Guo, Y. Han, H. Xiang, Y. Cheng, J. Xu, J. He and W. Zhang, *Mol. Psychiatry*, 2025, **30**, 3695–3707, DOI: 10.1038/s41380-025-02959-5.
8 S. Song, H. Zhou, X. Lan, X. Yuan, Y. Li, S. Huang, Z. Wang and J. Zhang, *Arabian J. Chem.*, 2023, **16**, 104949, DOI: 10.1016/j.arabjc.2023.104949.
9 Y. Wu, L. Pan, Z. Chen, Y. Zheng, X. Diao and D. Zhong, *Curr. Drug Metab.*, 2021, **22**, 838–857, DOI: 10.2174/1389200222666211006104502.
10 Y. Li, X. Lan, S. Wang, Y. Cui, S. Song, H. Zhou, Q. Li, L. Dai and J. Zhang, *Front. Pharmacol*, 2022, **13**, DOI: 10.3389/fphar.2022.1065654.
11 J. Li, Y.-J. Tan, M.-Z. Wang, Y. Sun, G.-Y. Li, Q.-L. Wang, J.-C. Yao, J. Yue, Z. Liu, G.-M. Zhang and Y.-S. Ren, *Br. J. Pharmacol.*, 2019, **176**, 1106–1121, DOI: 10.1111/bph.14595.
12 F. Zhang, Y. Yan, K. Ding, W.-W. Lian, L. Li, W.-P. Wang, C.-Y. Xia, H. Yang, J. He, W.-K. Zhang and J.-K. Xu, *J. Ethnopharmacol.*, 2024, **319**, 117130, DOI: 10.1016/j.jep.2023.117130.
13 J. Huang, S. Huang, J. Zhang, Y. Liang, J. Bai, W. Xu, L. Gong, H. Su, Z. Huang and X. Qiu, *J. Agric. Food Chem.*, 2022, **70**, 7773–7785, DOI: 10.1021/acs.jafc.2c00572.
14 K. Li, M. Liu, M. Zhang, Q. Li, K. Yu, J. Li, Z. Shang and W. Cai, *J. Pharm. Biomed. Anal.*, 2023, **233**, 115447, DOI: 10.1016/j.jpba.2023.115447.
15 K. Li, A. Tian, L. Shu, L. Zhu, C. Yang, Q. Li, S.-H. Liu, Y.-C. Cheng and W. Cai, *J. Chromatogr. A*, 2025, **1758**, 466181, DOI: 10.1016/j.chroma.2025.466181.
16 J. Guo, Y. Shang, X. Yang, J. Li, J. He, X. Gao and Y. Chang, *J. Chromatogr. A*, 2022, **1675**, 463172, DOI: 10.1016/j.chroma.2022.463172.
17 S.-H. Qin, Y. Xu, K.-L. Li, K.-Y. Gong, J. Peng, S.-L. Shi, F. Yan and W. Cai, *J. Anal. Methods Chem.*, 2021, **2021**, 6630604, DOI: 10.1155/2021/6630604.
18 Q. Du, Y.-X. Fu, A.-M. Shu, X. Lv, Y.-P. Chen, Y.-Y. Gao, J. Chen, W. Wang, G.-H. Lv, J.-F. Lu and H.-Q. Xu, *Life Sci.*, 2021, **272**, 118808, DOI: 10.1016/j.lfs.2020.118808.
19 X. Linli, Y. Mengmeng, L. Yanyan and Z. Yan, *Chin. J. Clin. Pharmacol.*, 2025, **41**, 366–371, DOI: 10.13699/j.cnki.1001-6821.2025.03.014.
20 H. Li, H. Wang, P. Dong, H. Li, S. Wang and J. Zhang, *Arabian J. Chem.*, 2024, **17**, 105597, DOI: 10.1016/j.arabjc.2023.105597.
21 X. Lan, Y. Li, H. Li, S. Song, X. Yuan, H. Zhou, Q. Chen and J. Zhang, *Arabian J. Chem.*, 2022, **15**, 104268, DOI: 10.1016/j.arabjc.2022.104268.
22 J. Jin, Q. Luo and F. Shi, *J. Chromatogr. B*, 2023, **1228**, 123861, DOI: 10.1016/j.jchromb.2023.123861.